Free-Form Fibers: A Whole Brain Fiber-to-DTI Registration Method

Chao Li[1,2], Xiaotian He[2,3], Vincent Mok[4], Winnie Chu[5], Jing Yuan[5], Ying Sun[1], and Xiaogang Wang[2,3]

[1] Department of Electrical and Computer Engineering,
National University of Singapore, Singapore 117576, Singapore.
[2] Shun Hing Institute of Advanced Engineering,
The Chinese University of Hong Kong, Hong Kong.
[3] Department of Electronic Engineering,
The Chinese University of Hong Kong, Hong Kong.
[4] Department of Medicine and Therapeutics,
The Chinese University of Hong Kong, Hong Kong.
[5] Department of Imaging and Interventional Radiology,
The Chinese University of Hong Kong, Hong Kong.

Abstract. We propose a novel whole brain fiber-to-DTI registration method and apply it to a clinical study of small vessel diseases. It deforms a manually annotated fiber model to diffusion tensor images of new subjects. Fiber trajectories and anatomically meaningful fiber bundles are automatically obtained by this registration. The free-form deformations are used to regularize the transformations at the whole brain level and across fiber bundles. Fiber curvatures are penalized as the intra-fiber regularization to encourage the smoothness of transformed fibers. A Laplace along-fiber regional prior learned from healthy subjects is proposed to evaluate the match between fibers and tensors in patients. It effectively improves the registration performance in the presence of white matter lesions. Experimental results show successful registration on 55 subjects and the DTI measurement computed from registered anatomical fiber bundles have significant correlation with cognitive functions.

1 Introduction

Diffusion Tensor Imaging (DTI) can characterize properties of white matter (WM) tissue in the brain and has great potentials in both clinical and neuroscientific studies. In many cases, scalar measures such as the fractional anisotropy (FA) are directly computed from diffusion tensors in the whole brain or in regions of interest for clinical and neuroscientific studies [1], whereas more advanced DTI measures with stronger statistical power require tractography [2, 3] or even tractography segmentation [4, 5]. However, tractography suffers from the problems of noise, partial volume effects, and early termination of fibers, especially when patients have white matter lesions. In tractography segmentation, it is difficult to obtain anatomically meaningful fiber bundles without human intervention.

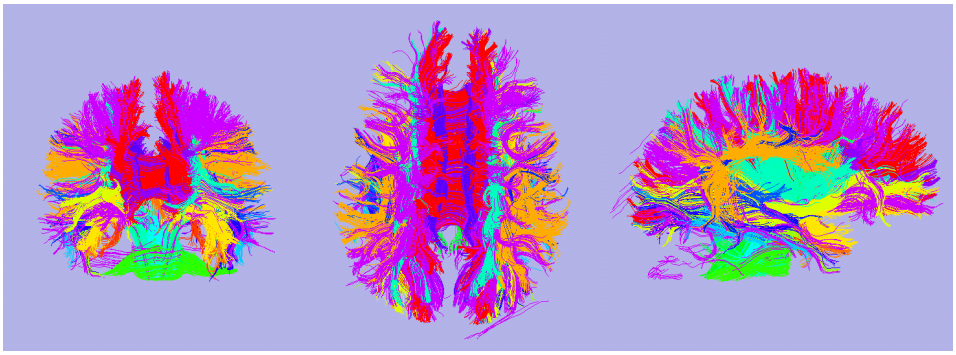

Fig. 1: Full brain fiber model. Different colors indicate different anatomical bundles.

Establishing the correspondences between fiber bundles and the pointwise correspondences along fibers in different subjects is also challenging.

We circumvent these challenges by directly registering a manually annotated whole brain fiber model to diffusion tensor images of new subjects. In the fiber model, outlier fibers are removed and the remaining fibers are labeled into well-known anatomical structures. This fiber-to-DTI registration scheme is attractive because it simultaneously achieves tractography and tractography segmentation after registration. The correspondences between fiber bundles and the pointwise correspondences along fibers across subjects are also automatically established. Moreover, it enforces the integrity of fibers and is robust to aforementioned DTI defects by using inter- and intra-fiber regularization. Additionally, DTI is fixed in fiber-to-DTI registration and thus the well-known problems of re-orientations and partial volume effects in DTI-to-DTI registration are avoided. Furthermore, fiber-to-DTI registration focuses on anatomical structures of interest and is less affected by other regions such as gray matter (GM).

This work is related to the active fibers approach [6], which deforms a chosen fiber bundle to match the diffusion tensor images by using the active contour model. Our work is distinct from [6] mainly in three aspects. Firstly, our fiber-to-DTI registration algorithm is able to register whole brain fibers simultaneously, whereas the active fibers method [6] only deals with a single bundle and is hence theoretically prone to local optima and may lead to physically impossible fiber bundle topology. Secondly, we model the deformations by free-form deformations (FFD) [7, 8], whose parameter number is independent of the number of fibers. On the contrary, the parameter number of [6] is proportional to the number of fibers, and therefore the regularization is much more complicated. Thirdly, we propose an along-fiber regional prior learned from healthy subjects to improve the performance of registration in the presence of WM lesions, and our algorithm has been applied to 31 healthy subjects and 24 patient subjects. In contrast, the similarity measure in [6] is purely the fiber-tensor fit measurement, which is very local and unreliable in the presence of WM lesions. Besides, the validation of [6] is only performed on 5 healthy subjects.

2 Free-Form Fibers (FFFs) Model

Our expert-annotated fiber model comprises of 20,000 tracts which are evenly sampled into 1,000,000 fiber points with a step of 0.5mm. The fiber model is obtained by first automatically clustering fibers into a large number of small bundles, then manually removing outlier bundles and merging bundles into anatomical structures (called anatomical fiber bundles). Finally there are 21 anatomical fiber bundles. The fiber model is shown in Fig. 1.

Let FT_i denote a serial of fiber points along the fiber tract i. The whole brain fiber model is construted by stacking all the fiber tracts:

$$\begin{aligned}\boldsymbol{P} =&[FT_1, FT_2, \cdots, FT_{\mathbb{T}}]^T \\ =&[\boldsymbol{p}_1^1, \boldsymbol{p}_1^2, \cdots, \boldsymbol{p}_1^{n_1}, \boldsymbol{p}_2^1, \boldsymbol{p}_2^2, \cdots, \boldsymbol{p}_2^{n_2}, \cdots, \boldsymbol{p}_{\mathbb{T}}^1, \boldsymbol{p}_{\mathbb{T}}^2, \cdots, \boldsymbol{p}_{\mathbb{T}}^{n_{\mathbb{T}}}]^T,\end{aligned} \tag{1}$$

where $\mathbb{T}$ is the total number of tracts, and n_i represents the number of points of tract i.

Given a mesh grid of control points $\boldsymbol{\Phi}$ with uniform spacing (n_x, n_y, n_z), the B-spline FFD maps a fiber point (x, y, z) to:

$$\boldsymbol{p}(x, y, z) = \sum_{l=0}^{3}\sum_{m=0}^{3}\sum_{n=0}^{3} B_l(u)B_m(v)B_n(w)\boldsymbol{\phi}_{i+l,j+m,k+n}, \tag{2}$$

where $i = \lfloor x/n_x \rfloor - 1$, $j = \lfloor y/n_y \rfloor - 1$, $k = \lfloor z/n_z \rfloor - 1$, $u = x/n_x - \lfloor x/n_x \rfloor$, $v = y/n_y - \lfloor y/n_y \rfloor$, $w = z/n_z - \lfloor z/n_z \rfloor$ and B is the B-spline basis function.

In FFFs, these B-spline coefficients represent the fiber points in the mesh coordinate system and are static during the evolution of $\boldsymbol{\Phi}$. Let $\boldsymbol{B}_{N\times M}$ denote the B-spline basis coefficient matrix. Equation (2) can be written as:

$$\boldsymbol{P}_{N\times 3}(\boldsymbol{\Phi}) = \boldsymbol{B}_{N\times M} \times \boldsymbol{\Phi}_{M\times 3}, \tag{3}$$

where N and M are numbers of fiber points and control points respectively.

Having this parametric model of the whole brain fibers, we find the deformations from the fiber model to the target brain DTI by optimizing the energy functional (4) with respect to $\boldsymbol{\Phi}$.

$$\begin{aligned}E(\boldsymbol{\Phi}) &= E_{\text{data}}(\boldsymbol{P}(\boldsymbol{\Phi})) + w_{\text{inter}}E_{\text{inter}}(\boldsymbol{\Phi}) + w_{\text{intra}}E_{\text{intra}}(\boldsymbol{P}(\boldsymbol{\Phi})) \\ &= E_{\text{data}}(\boldsymbol{B}\boldsymbol{\Phi}) + w_{\text{inter}}E_{\text{inter}}(\boldsymbol{\Phi}) + w_{\text{intra}}E_{\text{intra}}(\boldsymbol{B}\boldsymbol{\Phi}),\end{aligned} \tag{4}$$

where E_{data} is the data term which will be specified in Section 3; E_{inter} and E_{intra} are the inter- and intra-fiber regularization terms; w_{intra} and w_{inter} are experimentally chosen term weights. In [6], inter-fiber regularization is obtained by penalizing transformation difference of local connected fiber points while ignoring distances between fiber points. By contrast, we want to have control of the elasticity of the whole brain volume rather than only for the fiber points. So we penalize the bending energy term on the mesh as

$$E_{\text{inter}}(\boldsymbol{\Phi}) = \sum_i \sum_j \sum_k \|\nabla^2 \boldsymbol{\Phi}\|_F^2, \tag{5}$$

where $\|\cdot\|_F$ is the Frobenius norm. Note that $\boldsymbol{\Phi}$ here is a 3D vector field, whereas in (3) is the stacked version.

Although warping brain fibers with regularized deformations does not change the curvatures of fibers significantly, it is uncertain whether this change will compensate the curvatures of the input fibers or amplify them because the FFD models a solid volume [7] and is blind to fibers. Since low curvature is a common assumption on the brain fibers in most tractography approaches, we introduce the intra-fiber regularization term to encourage FFD to move towards the direction that will result in smooth fibers. We define

$$E_{\text{intra}} = \sum_s \|\Lambda \nabla^2 \boldsymbol{P}\|^2, \tag{6}$$

where Λ is a diagonal matrix that $\Lambda_{ss} = 0$ if point $\boldsymbol{p}_s$ is an end fiber point, and $\Lambda_{ss} = 1$ otherwise.

We minimized the energy functional by a quasi-Newton approach. The gradient is calculated as below:

$$\nabla_{\boldsymbol{\Phi}} E = \boldsymbol{B}^T (\nabla_{\boldsymbol{P}} E_{\text{data}} + \nabla_{\boldsymbol{P}} E_{\text{intra}}) + \nabla_{\boldsymbol{\Phi}} E_{\text{inter}}. \tag{7}$$

3 Similarity Measures

The fiber-DTI similarity measure is defined by the data term

$$E_{\text{data}}(\boldsymbol{P}) = w_{\text{DTI}} E_{\text{DTI}}(\boldsymbol{P}) + (1 - w_{\text{DTI}}) E_{\text{region}}(\boldsymbol{P}), \tag{8}$$

where E_{DTI} measures whether the majority of the principal diffusion directions of tensors are aligned with the tangents of fibers, and E_{region} is based on a regional prior that will be elaborated later in this section. Let $\boldsymbol{v}_s$ denote the unit tangent vector of point $\boldsymbol{p}_s$ on the deformed fiber tracts and $\boldsymbol{D}_s$ denote the tensor at $\boldsymbol{p}_s$. We define the data term as the **n**ormalized **Fi**ber-**T**ensor-fit(nFiT)

$$E_{\text{DTI}} = -\sum_s \frac{\boldsymbol{v}_s^T \boldsymbol{D}_s \boldsymbol{v}_s}{\text{tr}(\boldsymbol{D}_s)}. \tag{9}$$

When applied to patient subjects, using only the nFiT measurement is insufficient. On one hand, WM lesions may alter the microstructure of fiber tracts [9], making the nFiT measure unreliable. On the other hand, the tensor directions in a local area may be highly inconsistent due to the complexity of fiber structures. For instance, superior cingulum is perpendicular to corpus callosum but they are very close to each other. This complexity of fiber structures poses difficulty on quasi-Newton optimization. Owing to the inter- and intra-fiber regularization, the FFFs framework is able to overcome these limitations when used on most healthy subjects, but often fails on patient subjects due to the contamination of fiber tracts. Therefore, we enrich the data term by incorporating a regional prior learned from healthy subjects.

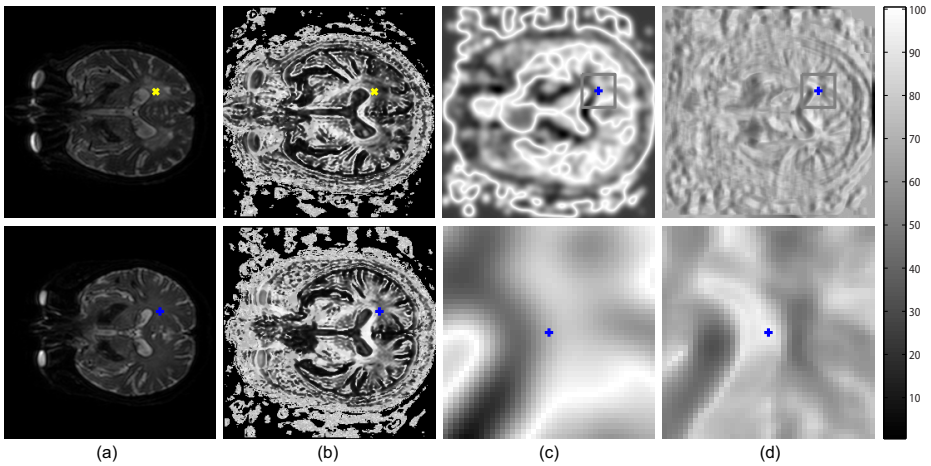

Fig. 2: Baseline (a) and FA (b) images for a patient subject (upper) and a healthy subject (lower); and similarity map for the '×' point obtained by diffused FA (c) and our region descriptor (d). '+' shows the correspondence of '×'. The lower row is the close up of the upper row for (c) and (d).

Extract regional features To learn the regional prior, we need a feature that does not vary much between healthy and patient subjects. However, most DTI features are not invariant to lesions, which is not surprising because the microstructure is altered. Nevertheless, boundaries between WM and GM are still clear in FA images despite the WM is darkened by lesions (see Fig. 2(b)). This observation motivates us to use a region descriptor to extract the regional FA feature for every fiber point.

The descriptor is defined as the correlation coefficients for a local window between FA and three positional features ($\kappa_1 = -y + z$, $\kappa_2 = x + y + z$, $\kappa_3 = -x + y + z$):

$$RCC(FA, \kappa_k) = \mathrm{cov}(FA, \kappa_k) / \sqrt{\mathrm{cov}(FA, FA)\mathrm{cov}(\kappa_k, \kappa_k)}, \tag{10}$$

where $\mathrm{cov}(A, B)$ is the covariance of A and B in a local window.

We choose these three positional features because they are fairly simple and fit the principal axis of the lateral ventricle of the majority of our data. Note that it is not necessary for the features to be exactly orthogonal.

As shown in Fig. 2, diffused (blurred) FA leads to low similarity at the corresponding point due to the reduction of FA value. On the contrary, our region descriptor generates high similarity at the corresponding point.

Actually, our 3-channel descriptor performs similar to edge detector but has the following three advantages. (1) Unlike the simple gradient which is computed from neighboring voxels, the region correlation is the statistics of a local region and is thus robust to noise; it is also invariant to the local average and variance of FA, the reduction of which is a common result of WM lesions. (2) Due to

the large overlap of neighboring windows, it diffuses the WM surface to its neighborhood which enlarges the capture range of the model. (3) These features can be computed very efficiently by using the integral image representation [10] whose complexity is independent of the window size.

Learn the features for patient subject registration After registration of healthy subjects using (9), we respectively learn the three features for every fiber point by Laplace distributions. This statistical along-fiber prior is very different from the conventional atlas which is based on a single reference image. The conventional atlas method deforms fibers according to image-to-image registration and accordingly any misalignment in the atlas will be propagated to the final result. Contrarily, in our framework, registration errors of a single training sample are regarded as outliers and will not affect the Laplace priors much.

We define the regional data term as

$$E_{\text{region}}(\boldsymbol{P}) = -\log p(\boldsymbol{P}; \kappa_1, \kappa_2, \kappa_3) \approx -\sum_s \log p(\boldsymbol{p}_s; \kappa_1) p(\boldsymbol{p}_s; \kappa_2) p(\boldsymbol{p}_s; \kappa_3)$$
$$= -\sum_s \sum_k \left(\frac{|RCC_s^k - \mu_s^k|}{b_s^k} + C(b_s^k) \right), \tag{11}$$

where μ_s and b_s are the location and scale parameters of Laplace distributions learned from registration results of healthy subjects. RCC_s^k is short for $RCC(FA, \kappa_k)$. $C(b_s^k)$ is a constant value independent of $\boldsymbol{P}$.

For healthy subjects, regional prior is not available and we set $w_{\text{DTI}} = 1$. For patient subjects, since the B-spline grid is optimized in a coarse-to-fine manner, we set $w_{\text{DTI}} = 0$ at coarse grid levels because the regional term is more robust, and $w_{\text{DTI}} = 0.5$ at the finest grid level, to balance the two terms and refine the registration results.

4 Results

24 elderly patients in various stages of Small Vessel Desease (SVD) are recruited for an experimental treatment. 31 healthy subjects are enrolled for reference. Diffusion weighted images (DWI) are acquired on a 3-T Philips Achieva MRI scanner (Philips, Netherlands) in 16 gradient orientations with field of view equal to $220 \times 220 \times 165$ mm^3 at the b-value of 750 s/mm^2. Pixel spacing equals to 0.86×0.86 mm^2 and the slice thickness is 3 mm. The repetition time/echo time equals to 10900/84.5. The finest B-spline control point spacing is about $7 \times 7 \times 6$ mm^3. Based on the visual validation of the major fiber bundles, the fiber-to-DTI registration is successful for all the 55 subjects.

Fig. 3 compares the corpus callosum constructed by manual seeded tractography (a) with three fiber-to-DTI registration approaches: (b) affine alignment; (c) FFFs with nFiT alone as the similarity measure ("nFiT" for short); and (d) FFFs with nFiT and the regional prior ("RCC-nFiT" for short). As shown in the upper row, due to WM lesions, the tractography approach (a) fails to reconstruct the middle part of the corpus callosum (CC), whereas integrity of the CC

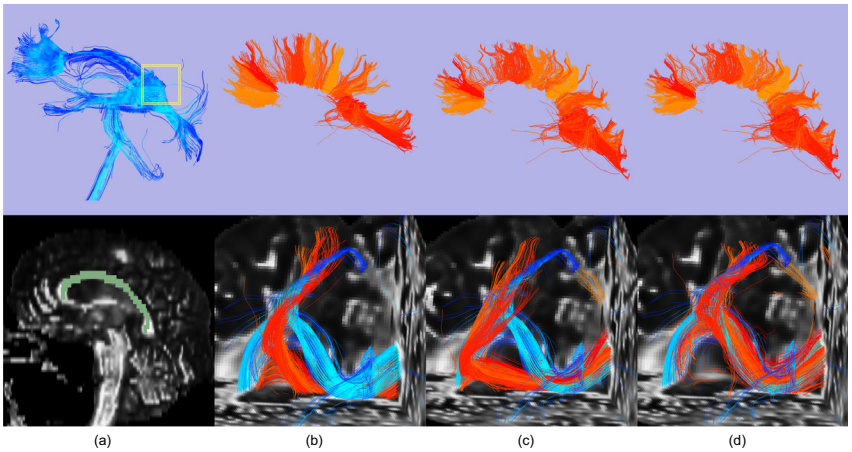

Fig. 3: The corpus callosum reconstructed by using manual seeding(a), affine alignment(b), nFiT(c), and RCC-nFiT(d). The lower figure of (a) shows the seed region.

is maintained in the fiber-to-DTI registration approaches (b-d). The lower row compares the tractography (white) and registration results (gray) in close-up view. If registration does well, the registered fiber template should match the fibers reconstructed from manually seeded tractography. After affine alignment, there is still shape mismatch between the tensor and the corresponding anatomical structure, i.e., the tractography result. The nFiT approach deformed the fiber in wrong direction while the residue mismatch was successfully corrected by RCC-nFiT.

The upper row of Fig. 4 displays the patient registration results in different depths. As shown, the registered fiber bundles well fitted the anatomical structures on the DTI data and the fiber bundles were able to go through the lesion regions (highlighted in white squares). It is important to note that by using an annotated fiber model, we are able to simultaneously segment multiple regions, e.g., inferior cerebellar peduncle in green, corpus callosum in magenta, and superior cingulum in blue. The lower row of Fig. 4 compares affine alignment, nFiT, and RCC-nFiT results. Anatomically, the corpus callosum (in cyan squares) should not cross the lateral ventricle (the central bright region). It is clearly shown that the RCC-nFiT approach outperformed the other two.

Since the key contribution of the work is to achieve fiber-to-DTI registration at whole brain scale which is too complex to synthesize, we are currently unable to validate the registration with ground truth. Alternatively, previous clinical studies [1] suggested that DTI measures should have strong correlations with cognitive impairment. We therefore validate our results by testing whether it is coherent with the clinical finding. Specifically, we test the partial correlation coefficients between the along-fiber nFiT and two widely used cognitive scores: the Mini-Mental State Examination (MMSE) and the Montreal Cognitive Assessment (MoCA), based on 24 patients with control for age, gender,

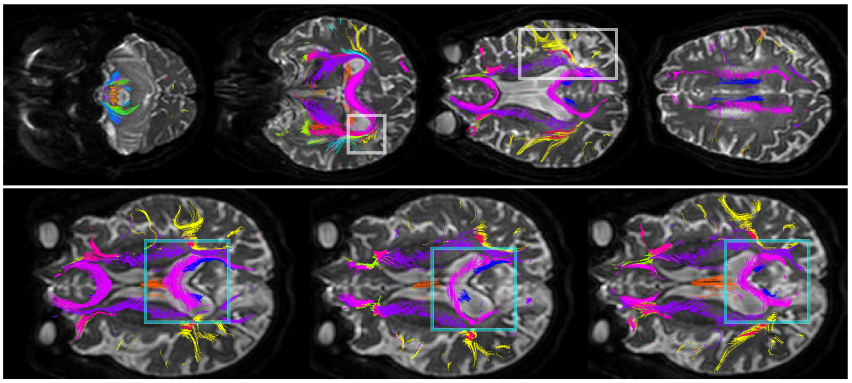

Fig. 4: Upper row: RCC-nFiT results of a patient subject in axial view. Lower row: comparison of results from affine alignment (left), nFiT (center), and RCC-nFiT (right). Points within the slice space are overlayed. View in color for fibers.

and education. As shown in Table 1, the correlation is remarkably improved by incorporating regional prior for both MMSE and MoCA. The p-value of the correlation between RCC-nFiT results and MoCA scores is 0.001, indicating that the along-fiber nFiT measure obtained by our fiber-to-DTI registration could be used as predictors of cognitive impairment.

	Affine	nFiT	RCC-nFiT
Correlation with MMSE	0.373	0.487	0.561
Correlation with MoCA	0.462	0.657	0.725

Table 1: Correlation coefficients between cognitive scores and along fiber measurements.

5 Conclusion

A novel whole brain fiber-to-DTI registration method, named free-form fibers (FFFs), is proposed and demonstrated to be able to automatically obtain whole brain fiber trajectories and annotation. Using a unique whole brain fiber model to match multiple subjects, the method provides inter-subject correspondence by nature, thus allowing for group analysis. Meanwhile, by using intra- and inter-fiber regularization, the method can avoid early termination of fibers, which is a vital limitation of the conventional tractography method. We also propose a Laplace regional prior that is learned from healthy subjects and makes the registration for SVD patients robust towards WM lesions. Experimental results showed successful registration for both healthy subjects and SVD patients and demonstrated improvement by using regional prior. Similar conclusion is con-